

Optimization of Spraying Parameters for Hydroxyapatite

Gross K. A.

Latvian Scientific Research Institute of Traumatology and Orthopaedics,
Riga/USSR

Berndt C. C.

State University of New York, Stony Brook, NY/USA

ABSTRACT

Hydroxyapatite (HAp) is sprayed for bioceramic applications; for example to apply a coating to the stem of a hip prosthesis that enables enhanced fixation and stabilization to the body. A prime difficulty in the preparation of thermally sprayed coatings is formal assessment of the coating structure. This aspect of coating preparation is addressed in the present paper.

The nature of the coating morphology, composition and crystallinity change with respect to the stand-off distance, the particle size, and the power level of the plasma spraying process. The above processing parameters have been systematically varied. The quality of the coating has then been given a relative index. This simple procedure allows the rapid determination of processing/morphology relationships within thermally sprayed materials so that optimum parameters can be determined. The quality of low pressure plasma sprayed coatings is also reported and discussed.

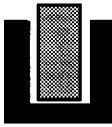
1. INTRODUCTION

Ceramics that can be used for substitution within the body may be termed as bioceramics. Bioceramics are usually favoured over other materials because their composition mimics the body more closely than polymers or alloys. They offer one of the following responses. They can behave as an inert ceramic exhibiting very little dissolution, as a biotolerant ceramic which is separated from the body by a fibrous capsule, as a surface-active ceramic which forms a very strong biological bond after a small amount of dissolution or, as a resorbable ceramic which completely dissolves within a predestined time [1]. The body reaction to these separate ceramic classes is depicted in Figure 1.

A bioceramic of the bioinert or surface reactive class are the most favoured [2] for applications of hip prostheses where fixation is necessary. Biotolerant implants exhibit weak interfacial strengths and resorbable ceramics are not used due to the inability of the femur to reconstruct itself as the ceramic dissolves. Bioinert ceramics with porous surfaces can allow the bone to grow up to the implant and form a mechanical bond [3]. This type of fixation mechanism is used widely but offers a lower bond strength than hydroxyapatite. Hydroxyapatite, a ceramic of the surface active class, is thought to be an ideal bone substitute, because the material becomes integrally involved in the bone metabolism and is gradually resorbed as the bone is remodelled [4].

Coating techniques such as hot isostatic pressing, electrophoretic deposition, physical vapour deposition, frit enamelling and sol-gel deposition have all been used to produce HAp coatings but plasma spraying is the most promising [5]. Plasma sprayed hydroxyapatite coatings with different porosities and compositions have been produced; however there is little data available which enables a direct comparison between processing and microstructure so that optimum thermal spraying parameters can be ascertained.

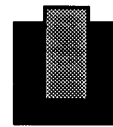
i) Bioinert



a) Insertion of implant into body.

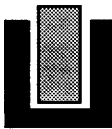


b) Bone regenerates and grows to fill the gap.

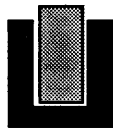


c) Bone grows up to and contacts implant.

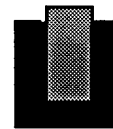
ii) Biotolerant



a) Insertion of implant into body.



b) Bone grows up to implant.



c) Bone does not bond to implant. Fibrous capsule forms.

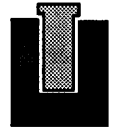
iii) Surface Active



a) Insertion of implant into body.



b) Dissolution of surface layers.

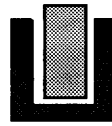


c) Bone growth up to surface of implant.

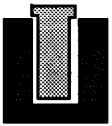


d) Formation of biological bond.

iv) Bioresorbable



a) Insertion of implant into body.



b) Bone growth up to implant. Dissolution of implant begins.



c) Resorption of implant and bone growth.



d) Complete replacement of implant by bone.

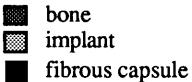
Key:  bone
implant
fibrous capsule

Figure 1. Behaviour of (i) bioinert, (ii) biotolerant, (iii) surface active and (iv) bioresorbable biomaterials when implanted into osseous tissue of a person or an animal.

2. EXPERIMENTAL PROCEDURES

2.1 Powder Production

The powders used in the present study were prepared by the wet method. Powder preparation was carried out by adding 27 litres of 0.3M orthophosphoric acid to 27 litres of 0.5M calcium hydroxide solution. The temperature of the calcium hydroxide solution was 40°C while the orthophosphoric acid was added in a dropwise fashion over 3 hours. A gelatinous

precipitate results; this was allowed to settle and then the clear liquid decanted. The remaining water is removed by placing the gelatinous precipitate in an oven at 180°C. After about 20 hours of drying, the resultant cake is attrited in a mortar to obtain powder of the desired particle size. Dry sieving was used to obtain various size ranges of hydroxyapatite. Powder fractions used include 25-44 µm, 44-55 µm, 55-85 µm and 85-95 µm. The powder was then calcined at 800°C for two hours and then cooled in an oven which was set to 80°C.

2.2 Thermal Spraying

2.2.1 Atmospheric Plasma Spraying

Hydroxyapatite powder was transported to the plasma torch by a Metco 3MP mechanical powder feeder. High purity argon at a flow rate of 30 l/min was used to carry the powder at about 3 g/min.

Plasma-arc spraying was performed with a Plasmadyne system and arc gases of argon and helium set to 345 kPa at 45 l/min and 413 kPa at 10 l/min respectively. A robotic arm was employed to move at a constant speed across the surface so that a coating of uniform thickness could be deposited. Compressed air cooling was used to keep the substrate at a low temperature and to avoid the inclusion of small particles into the coating.

The dimensions of the mild steel substrates were 30 x 20 x 3 mm. These coupons were fixed onto seats which were positioned at various distances from the table surface. The mild steel substrates were steel grit blasted before spraying. The power level of the plasma spray gun was varied by changing the current. Current levels of 500, 700 and 900 A correspond to power levels of 13, 25 and 34 kW. Coatings could thus be obtained by using various cuts of hydroxyapatite powder at different spraying distances and power levels. Table 1 summarizes the plasma spraying variables and also indicates the corresponding coupon designation.

Table 1. Plasma spray variables and coupon designation used for manufacturing hydroxyapatite coatings.

Particle size (microns)	Power level (kW)	Stand off distance (cm)										
		5	7.5	10	12.5	15	20	22.5	25	27.5	30	32.5
85-95	34	14a	14b	14c	14d	14e	14f	-	-	-	-	-
"	25	15a	15b	15c	15d	15e	15f	-	-	-	-	-
55-85	34	5a	5b	5c	5d	5e	5f	5g	5h	5i	5j	5k
"	25	6a	6b	6c	6d	6e	6f	6g	6h	6i	6j	6k
"	13	7a	7b	7c	7d	7e	7f	-	-	-	-	-
44-55	34	12a	12b	12c	12d	12e	12f	-	-	-	-	-
"	25	13a	13b	13c	13d	13e	13f	-	-	-	-	-
25-44	34	8a	8b	8c	8d	8e	8f	8g	8h	8i	8j	8k
"	25	9a	9b	9c	9d	9e	9f	-	-	-	-	-
"	13	10a	10b	10c	10d	10e	10f	-	-	-	-	-
"	10	11a	11b	11c	11d	11e	11f	-	-	-	-	-

2.2.2 Low Pressure Plasma Spraying

Stainless steel coupons with dimensions of 31 x 41 x 3 mm were plasma sprayed under varying conditions. The substrates were roughened by grit blasting. The plasma spray gun was set to 28 kW and a hydroxyapatite powder sized to 25-44 µm was used as the source powder. The gun was positioned 25 cm from the substrate. Chamber pressure, arc gas flow, powder feed rate and exposure time was varied in accordance to the conditions shown in Table 2.

Table 2. Conditions used for low pressure plasma spraying hydroxyapatite.

Sample no.	Chamber pressure (torr)	Arc gas flow (slpm)	Powder Feed (g/min)	Exposure Time (min)
1	50	20	0.75	1.0
2	50	20	0.20	5.0
3	100	20	0.75	1.0
4	100	20	0.20	5.0
5	200	20	0.20	5.0
6	200	20	0.75	1.0
7	100	30	0.20	5.0
8	100	30	0.75	1.0
9	100	30	0.20	5.0
10	100	30	0.75	1.0
11	100	10	0.75	1.0
12	100	10	0.20	5.0

2.3 Characterization

X-ray diffraction was used to determine the phases present in the coating. The diffractometer was set for a continuous scan with a scan speed of 2°/min between 20 and 60 degrees. This allows the detection of calcium phosphate phases. The current and voltage were set to 30 mA and 30 V respectively; using Cu K α radiation. Scanning electron microscopy was used for examination of the microstructure. The coatings were sputter coated with gold and an acceleration voltage of 10 kV avoided excessive charging of the hydroxyapatite. Roughness measurements were performed with a Rank Taylor Hobson Surtronic 3P instrument. An average of 8 measurements will be reported in this work. Thermal analysis in an air atmosphere was performed on the powder and coating. A ramp rate of 10°C/min was used and the material heated to 1450 °C.

2.4 Mechanical Testing

The tensile adhesion test (ASTM C633-69) was used as a basis of determining the bond strength. Hydroxyapatite coatings were produced on 316 stainless steel and Ti-6Al-4V substrates and a cylinder of identical geometry fixed to the coating using FM73 epoxy adhesive. The assembly was then placed in a screw driven Instron and tested until failure. The fracture toughness of hydroxyapatite coatings were determined using a four point bend specimen with a groove in the coating. This 1.5 mm deep groove was produced by removing a part of the coating in a surface grinding operation. Two bars were then fixed together with FM73 epoxy adhesive and the assembly subjected to a four point bend test until failure occurred.

3. RESULTS AND DISCUSSION

3.1 Powder Characterization

Hydroxyapatite powder was produced with some tri-calcium phosphate impurities; this is not unusual and it has been found in some commercially available hydroxyapatite powders. Tri-calcium phosphate of the beta phase is readily formed if stringent processing conditions are not observed in the production stage. Calcining of the HAp powder results in colour changes from white to light blue and pink. These colour changes have been attributed to manganese ions in the lattice [6]. Although the very minor manganese impurities, of the order of ppm, do not influence the biocompatibility of the HAp; they may be detrimental to acceptance of the material by the customer. X-ray diffraction of the material in the as-received and post-calcined conditions indicated that the calcined material was more crystalline, Fig. 2.

The amount of HAp of the desired size fraction was less than 40% after the solid cake was crushed in the mortar and passed through 85 μ m and 25 μ m sieves. A sieving time of about 10 hours was necessary to remove fine particles (< 2 μ m) which adhered to the larger particles, Fig. 3. The morphology of the powder ranged from rounded to jagged. A shorter drying

history resulted in a rounded morphology since moisture remaining in the powder allowed rounding of the particles in the sieving operation.

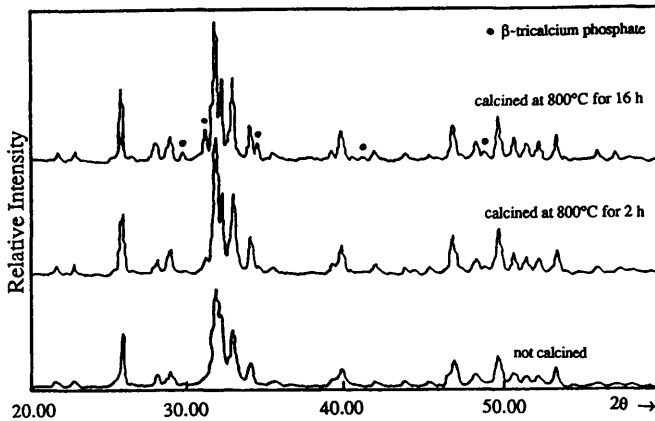


Figure 2. The change in crystallinity on calcining hydroxyapatite powder at 800 °C for 2 and 16 hours.

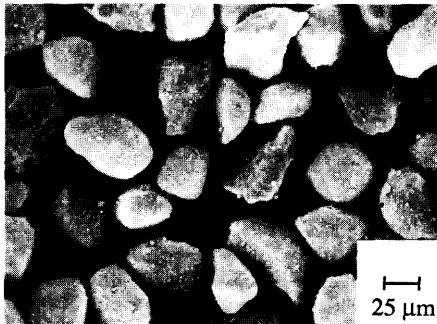


Figure 3. Adhesion of hydroxyapatite dust on larger particles.

3.2 Assessment of microstructure

3.2.1 Atmospheric pressure plasma sprayed coatings

The coating quality was assessed via SEM. The main focus of attention was on the extent of melting that could be qualitatively determined from the percentage of total surface area covered by well formed splats. Four types of microstructures were distinguished in atmospherically plasma sprayed coatings and these are categorized as follows:

- Type A: surface molten, cracked coating (Figure 4a)
- Type B: partially molten coating with a few splats (Figure 4b)
- Type C: coating with good splat formation (Figure 4c)
- Type D: coating with respheroidized droplets (Figure 4d)

The cracked coating shown in Figure 4a results when the substrate is close to the plasma torch (< 6.0 cm). Thus the coating was surface fused after powder deposition and excessive cracking occurs due to large thermal expansion differences between the coating and substrate. Typical crack widths are about 0.1 μm for plasma sprayed coatings but sample 4a exhibited cracks which were 1 μm wide. These cracks penetrate to the substrate and allow the coating to remain intact by establishing a segmented crack network.

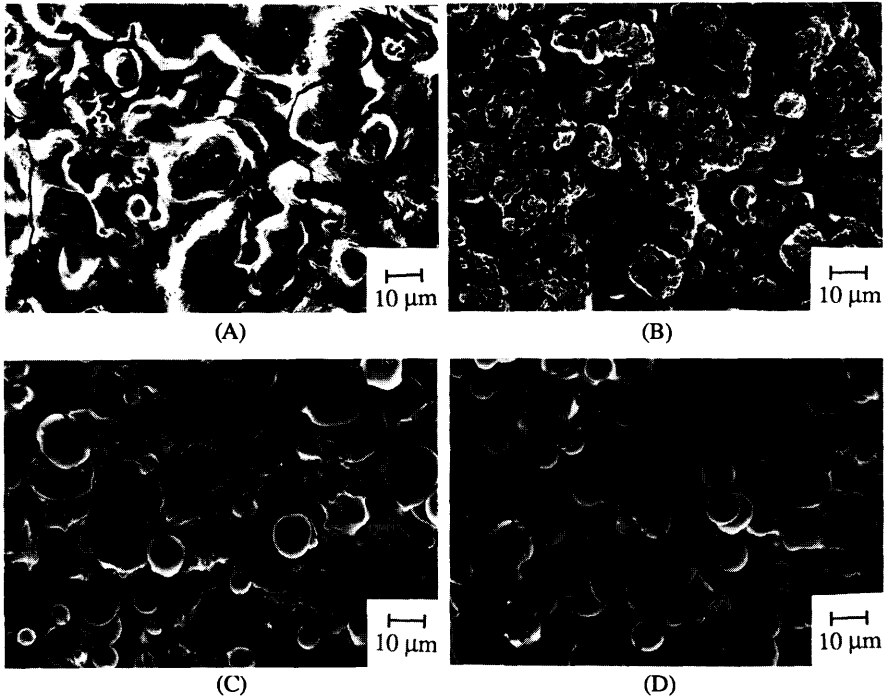


Figure 4. Characteristic coatings observed during the plasma spraying of hydroxyapatite. The four types include (A) a surface molten and cracked coating, (B) a partially molten coating with a few splats observed, (C) a coating with good splat formation and (D) a coating with molten and respheroidized droplets.

Changes in the stand-off distance and the power level influence the microstructure. Coatings with good splat formation can only be obtained for a small range of stand-off distances at a particular power level. As the power level decreases, the stand-off distance is decreased to retain the desired morphology. The coating porosity however undergoes an increase as the power level is decreased. Figure 5 indicates how the coating morphology can be graphically related to the plasma spraying variables. An index system for the microstructure, Figure 4 described previously, has been used so that the optimum plasma parameters can be ascertained. The index was determined by visual inspection of SEM micrographs, and where there is a combination of two features, a fractional index was assigned. Figure 5a shows that an increase in power level from 13 kW to 34 kW should be coupled with an increase in stand-off distance from 17.5 to 22.5 cm, in order to produce the optimum microstructure as depicted by the index C (Fig. 4c).

The microstructure is also dependent on particle size. For example, Figure 5b shows that the spraying distance is reduced for a lower sized fraction of HAP powder; as would be expected since smaller particles require less time in the plasma effluent to completely melt.

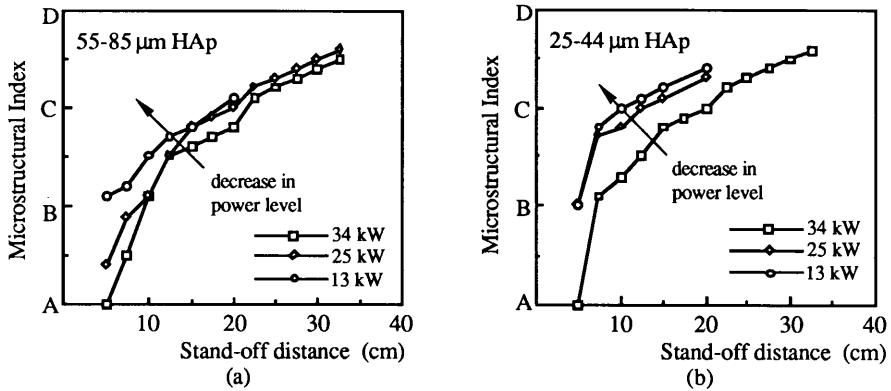


Figure 5. Influence of power level and stand-off distance on the coating quality for particle size distributions of (a) 55-85 μm and (b) 25-44 μm .

The thermal spraying conditions which produce a good surface morphology are given in Table 3 for different power levels and particle sizes. The powder cuts of 85-95 μm and 44-55 μm were not intensively investigated and only general details are shown in this work.

Table 3. Plasma spray parameters for good coating morphology. The stand-off distances for specific power levels and particle size cuts are indicated.

Particle size (μm)	Power level (kW)			
	35	25	13	10
85 - 95	> 20	> 20	-	-
55 - 85	22.5 - 25.0	20.0 - 22.5	20.0	-
44 - 55	> 20.0	20.0	-	-
25 - 44	15.0 - 20.0	12.5 - 15.0	10.0 - 12.5	10.0 - 12.5

The degree of particle melting was also identified from roughness measurements. A smoother coating implies that the particles reach a more fluid state and are able to spread on impact against the substrate. The roughness measured from coatings produced at increasing stand-off distances showed reproducible behaviour at lower power levels, Fig. 6. The molten surface that was observed at 35 kW and a 5 cm stand-off distance displayed a low initial roughness. Roughness then increased, Fig. 6, and this corresponds to particles which do not melt. By further increasing the stand-off distance the roughness decreased to a minimum where good splat formation was observed. The well formed splats correspond to droplets that have spread on the substrate and this results in a smooth surface. At larger stand-off distances the roughness increased again which agrees well with the onset of respheroidization. The minimum roughness measurement shifted to lower values by using powder of a smaller cut (eg., 25-44 μm in size).

Porosity would be minimized in a coating where good splat formation is observed. Moving away from this condition produces an increase in bulk and surface porosity. For example, bulk porosity would arise from the inability of the partially molten droplets to mould onto the irregular surface as smaller spraying distances are selected. The same problem arises as the spraying distance is increased because the spherical droplets resolidify. The distinction between these conditions is that in the former case the surface of the particle is irregular but molten. In the latter case the surface has begun to solidify and forms a shell.

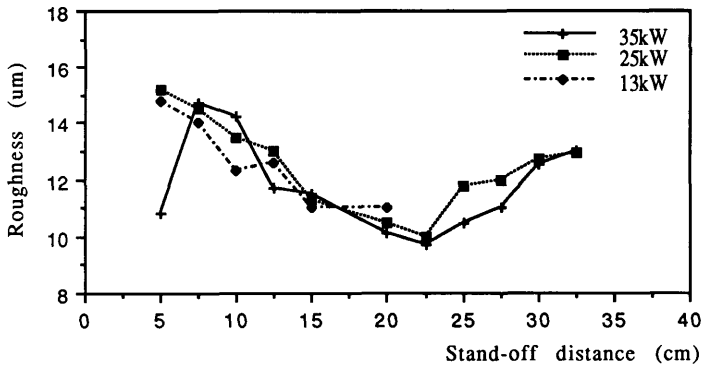


Figure 6. Roughness changes with increasing stand-off distances for power levels of 35 kW, 25 kW and 13 kW. A 55-85 μm powder was used in the spraying operation. The standard deviation is about $\pm 1 \mu\text{m}$.

3.2.2 Low pressure plasma sprayed coatings

The microstructures of low pressure plasma sprayed coatings are more consistent than those produced by atmospheric plasma spraying. Microstructures varied from either a rough unmolten appearance to a partially molten appearance. More splat formation was observed when the powder feed rate was set to 0.2 g/min. The roughness traces, Fig. 7, show that a smoother coating is produced by either increasing the chamber pressure or decreasing the plasma gas flow rate. The coatings de-adhered from some specimens.

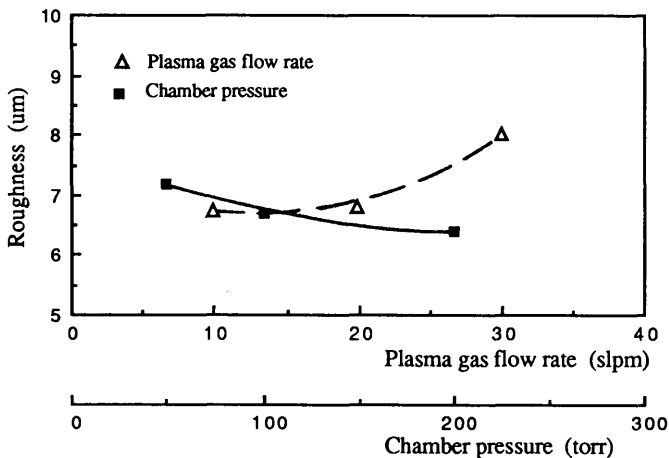


Figure 7. Roughness change with chamber pressure and plasma gas flow rate.

3.3 Chemical Phases and Crystallinity

The chemical phases of the coating change with the stand-off distance, power level and particle size. Four phases in total are observed and these are hydroxyapatite, calcium oxide, and beta and alpha phases of tricalcium phosphate. Coatings with a high percentage of HAp are produced when large particle sizes are used in conjunction with short stand-off distances. The amount of alpha and beta tri-calcium phosphate increases with the stand-off distance. The tri-calcium phosphate phases are biocompatible but resorb within the body leaving a porous coating. The effect of tri-calcium phosphate on the formation of the coating is unknown. A

different coefficient of thermal expansion of tri-calcium phosphate suggests that it could influence the coating quality. A smaller particle size (25-44 μm) encourages a further transformation to calcium oxide. The coatings that contain calcium oxide indicate that a high temperature transformation has taken place. A minor amount of tetracalcium phosphate is also observed.

Coatings exhibit increasing amorphicity with larger spraying distances and lower power levels. The change in amorphicity is more evident as the stand-off distance is increased, Fig. 8. It is difficult to resolve the peaks at stand-off distances of greater than 20 cm.

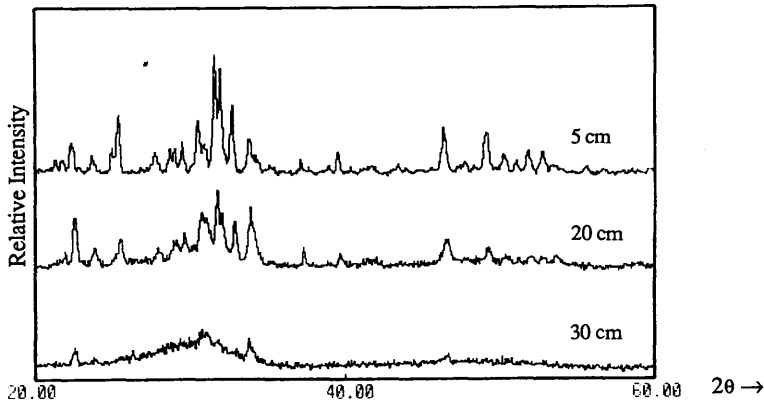


Figure 8. X-ray diffraction spectrum showing decrease in peak heights with stand-off distance.

A rounded peak, spanning a range of 4° , is positioned where the main peaks for hydroxyapatite, tricalcium phosphate and tetracalcium phosphate usually appear. Decreasing the power level leads to an decrease in crystallinity, Fig. 9. Residual stresses were found in the coatings as a shift to lower angles in the x-ray diffraction traces.

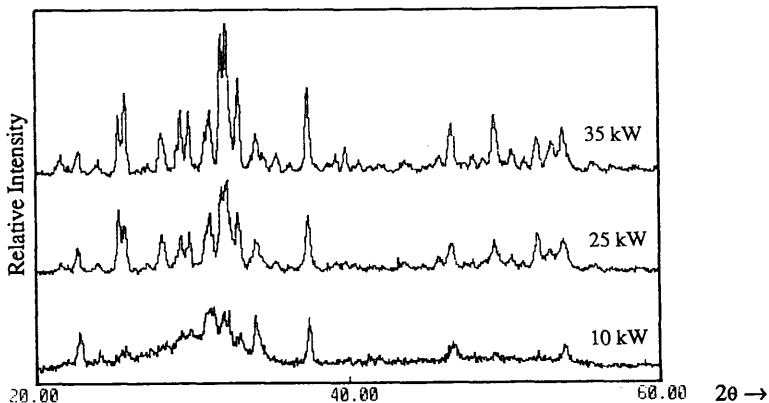


Figure 9. X-ray diffraction pattern showing decrease in peak heights with power level.

Coatings produced at lower power levels are undesirable because their increased porosity leads to a lower strength. These amorphous coatings are also undesirable since they are rapidly resorbed [7].

Heat treatment of amorphous coatings at 800°C for 2 hours shows a four fold rise in peak height suggesting an increase in crystallinity, Fig. 10. The tricalcium and tetracalcium phases are no longer detected by x-ray analysis in the heat treated coating. A trace of calcia is observed but this can be avoided by using a more pure hydroxyapatite powder. DTA curves for the powder and the amorphous coating show a difference in thermal behaviour, Fig. 11. The powder releases moisture at 100 °C. The powder is reasonably stable and similar to the coating in that it shows phase changes above 725 °C.

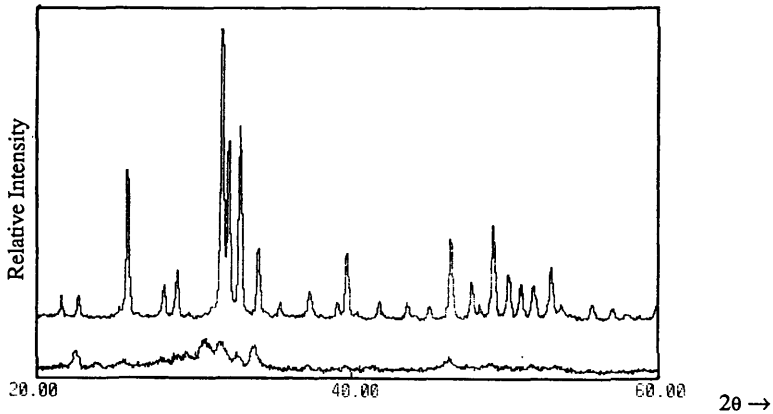


Figure 10. Increase in peak height after heat treatment of specimen 5g.

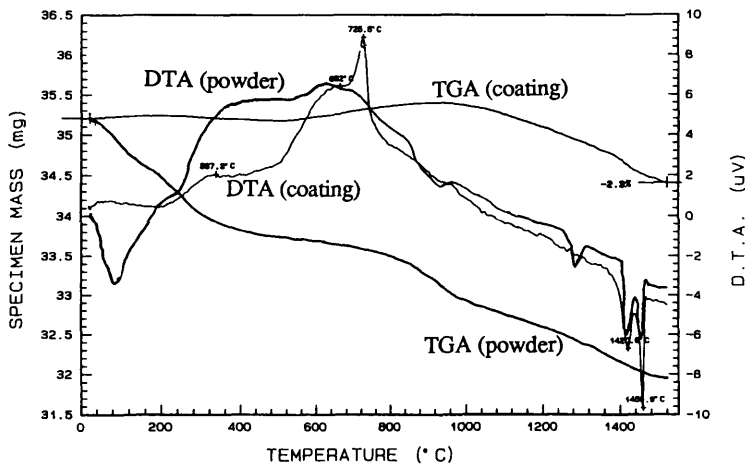


Figure 11. DTA/TGA analysis of source powder and specimen 5g. Heating rate is 10 °C/min.

Heat treatment of the coating results in morphological changes. The crack size increases after heat treating at 800 °C for 2 hours, Fig. 12. This is believed to result from the release of residual stresses which takes place within the coating.

Low pressure plasma sprayed coatings contained hydroxyapatite as the main phase. Alpha tricalcium phosphate was detected as the second major phase and traces of beta tricalcium phosphate and tetracalcium phosphate were identified. The phases were semi-crystalline and no crystallinity changes could be ascribed to the effect of changing conditions.

Coatings produced under the conditions of 5g (Table 1) were tested for fracture toughness. A range between 0.7 and 1.1 MPa.m^{-0.5} suggests that resistance to crack propagation is identical to dense hydroxyapatite bodies (0.7-1.0 MPa.m^{-0.5}) [10]. Failure occurred at the coating/substrate interface due to poor alignment of the fracture toughness specimens.

4. CONCLUSIONS

Manufacture of high grade hydroxyapatite powders requires well-controlled chemical processing techniques. The formation of hydroxyapatite in solution can be accompanied by the formation of tri-calcium phosphate if stringent chemical equilibrium conditions are not obeyed. A plasma sprayable powder can be produced by crushing and further sieving the dried hydroxyapatite precipitate.

Hydroxyapatite can be plasma sprayed successfully without the need of a bond coat. Some recommended plasma processing conditions for a particle size range of 55-85 µm are a spraying distance of 20.0 and 22.5 cm for corresponding power levels of 25 and 34 kW. A phase transformation to calcia occurs for size ranges of a lesser cut and such coatings are not recommended for implantation purposes. A porous surface can be manufactured where bone ingrowth into an implant is required. The porosity can be changed by altering the spraying distance and the power level. Crystallinity decreases with power level and stand-off distance but this can be solved by heat treating at 800 °C. Low pressure plasma sprayed coatings may not show promise due to restricted melting of the powder but this aspect of plasma processing requires further investigation.

ACKNOWLEDGEMENTS

The authors wish to thank the CSIRO/Monash University Collaborative Grant Fund that has enabled much of this work to be performed. Karlis Gross was supported by a Monash Research Scholarship.

REFERENCES

- 1) Boretos, J.W.: *Ceramic Bulletin*, 1985, **64** (8), 1098.
- 2) Kwarteng, K.B.: *SAMPE Q.*, 1988, **20** (1), 28-32.
- 3) Smith, T.S.: *SAMPE J.*, 1985, **21** (3), 14-16.
- 4) Kurosawa, H., Iwano, T. and Murase, K.: *Mater. Sci. Forum*, 1988, **34-36**, 363.
- 5) Berndt, C.C., Haddad, G.N., Farmer, A.J.D. and Gross, K.A.: *Materials Forum*, 1990, **14**, 161-173.
- 6) Johnson, P.D., Prener, J.S. and Kingsley, J.D.: *Science*, 1963, **141**, 1179.
- 7) Harris, D.H.: 3rd National Spray Conference, 1990, T13 of conference programme.
- 8) De Groot, K., Geesink, R., Klein, C.P.A.T. and Serekian, P.: *J. Biomed. Mater. Res.*, 1987, **21**, 1375.
- 9) Gitzhofer, F., Boulos, M.I., Filiaggi, M. and Pilliar, R.M.: 7th Cimtec World Ceramic Congress, Ceramics in Substitutive and Reconstructive Surgery, Italy, 1990, 113.
- 10) Akao, M., Aoki, H. and Kato K.: *J. Mater. Sci.*, 1981, **16**, 809-812.